

Excited state dynamics in DNA double helices

Eric R. Bittner*

Department of Chemistry and the Texas Center for Superconductivity, University of Houston, Houston TX 77204
(Dated: February 6, 2008 Available as: cond-mat/0606333)

Recent ultrafast experiments have implicated intrachain base-stacking rather than base-pairing as the crucial factor in determining the fate and transport of photoexcited species in DNA chains. An important issue that has emerged concerns whether or not a Frenkel exciton is sufficient one needs charge-transfer states to fully account for the dynamics. In we present an $SU(2) \otimes SU(2)$ lattice model which incorporates both intrachain and interchain electronic interactions to study the quantum mechanical evolution of an initial excitonic state placed on either the adenosine or thymidine side of a model B DNA poly(dA).poly(dT) duplex. Our calculations indicate that over several hundred femtoseconds, the adenosine exciton remains a cohesive excitonic wave packet on the adenosine side of the chain where as the thymidine exciton rapidly decomposes into mobile electron/hole pairs along the thymidine side of the chain. In both cases, the very little transfer to the other chain is seen over the time-scale of our calculations. We attribute the difference in these dynamics to the roughly 4:1 ratio of hole vs. electron mobility along the thymidine chain.

Give the importance of DNA in biological system and its emerging role as a scaffold and conduit for electronic transport in molecular electronic devices, [1] DNA in its many forms is a well studied and well characterized system. What remains poorly understood, however, is the role that base-pairing and base-stacking plays in the transport and migration of the initial excitation along the double helix.[2, 3] Such factors are important since the UV absorption of DNA largely represents the weighted sum of the absorption spectra of it constituent bases whereas the distribution of lesions formed as the result of photoexcitation are generally not uniformly distributed along the chain itself and depend strongly upon sequence, suggesting some degree of coupling between bases.[3]

Recent work by various groups has underscored the different roles that base-stacking and base-pairing play in mediating the fate of an electronic excitation in DNA. [2, 3] Over 40 years ago, Löwdin discussed proton tunneling between bases as a excited state deactivation mechanism in DNA[4] and evidence of this was recently reported by Schultz *et al.* [5] In contrast, however, ultrafast fluorescence of double helix poly(dA).poly(dT) oligomers by Crespo-Hernandez *et al.*[2] and by Markovitsi *et al.* [3] give compelling evidence that base-stacking rather than base-pairing largely determines the fate of an excited state in DNA chains composed of A and T bases with long-lived intrastrand states forming when ever A is stacked with itself or with T. However, there is considerable debate regarding whether or not the dynamics can be explained via purely Frenkel exciton models [6, 7, 8] or whether charge-transfer states play an intermediate role. [9]

Here we report on a series of quantum dynamical calculations that explore the fate of a localized exciton placed on either the A side or T side of the B DNA duplex poly(dA)₁₀.poly(dT)₁₀. Our theoretical model is based upon a $SU(2) \otimes SU(2)$ lattice model consisting of localized hopping interactions for electrons and holes be-

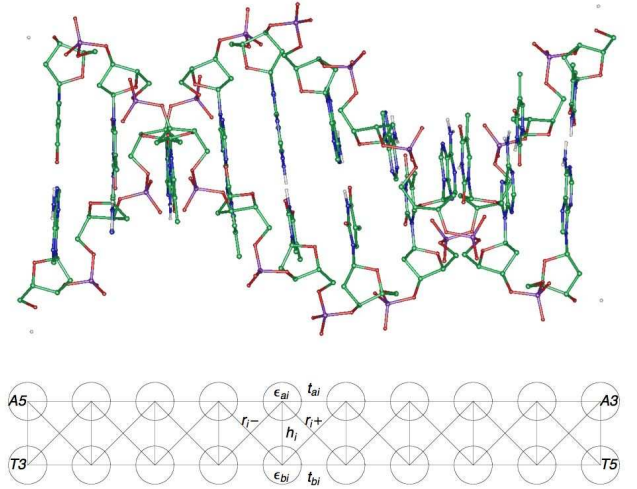


FIG. 1: Three dimensional structure of poly(dA)poly(dT) in the B DNA double helical form. This is considered to be the average structure in water. Bottom: Equivalent lattice model showing the connectivity and associated transfer terms.

tween adjacent base pairs along each strand (t_{aj}) as well as cross-strand terms linking paired bases (h_i) and “diagonal” terms which account for the π stacking interaction between base j on one chain and base $j \pm 1$ on the other chain (r_j^\pm) in which r_j^- denotes coupling in the 5'-5' direction and r_j^+ coupling in the 3'-3' direction. Fig. 1 shows the three-dimensional structure of poly(dA)₁₀.poly(dT)₁₀ and the topology of the equivalent lattice model. Taking link in this figure as a specific electron or hole hopping term, we arrive at the following single particle Hamiltonian,

$$h_1 = \sum_j \epsilon_j \hat{\psi}_j^\dagger \hat{\psi}_j + t_j (\hat{\psi}_{j+1}^\dagger \hat{\psi}_j + \hat{\psi}_j^\dagger \hat{\psi}_{j+1}) + h_j \bar{\psi}_j \hat{\psi}_j + \hat{\psi}_{j+1}^\dagger (r_j^+ \hat{\gamma}_+ + r_j^- \hat{\gamma}_-) \hat{\psi}_j + \hat{\psi}_j^\dagger (r_j^+ \hat{\gamma}_+ + r_j^- \hat{\gamma}_-) \hat{\psi}_{j+1}, \quad (1)$$

where $\hat{\psi}_j^\dagger$ and $\hat{\psi}_j$ are $SU(2)$ spinors that act on the ground-state to create and remove an electron (or hole) on the j th adenosine or thymidine base along the chain. The $\hat{\gamma}$ operators are the 2×2 Pauli spin matrices with $\hat{\psi}_j = \hat{\gamma}_1 \hat{\psi}_j^\dagger$ and $\hat{\gamma}_+ + \hat{\gamma}_- = \hat{\gamma}_1$ providing the mixing between the two chains. Taking the chain to homogeneous and infinite in extent, one can easily determine the energy spectrum of the valence and conduction bands by diagonalizing

$$\hat{h}_1 = \begin{pmatrix} \epsilon_a + 2t_a \cos(q) & h + r^+ e^{-iq} + r^- e^{+iq} \\ h + r^+ e^{+iq} + r^- e^{-iq} & \epsilon_b + 2t_b \cos(q) \end{pmatrix} \quad (2)$$

where $\epsilon_{a,b}$ and $t_{a,b}$ are the valence band or conduction band site energies and intra-strand hopping integrals. When $r_j^+ = r_j^-$, Eq. 2 is identical to the Hamiltonian used by Creutz and Horvath [10] to describe chiral symmetry in quantum chromodynamics in which the terms proportional to r are introduced to make the “doublers” at $q \propto \pi$ heavier than the states at $q \propto 0$.

The coupling between the conduction and valence bands is accomplished by introducing short-ranged Coulomb and exchange interactions as well as “dipole-dipole” terms which couple geminate electron-hole pairs on different sites.

$$H(12) = h_1 + h_2 + \sum_{\mathbf{m}, \mathbf{n}} V_{\mathbf{m}, \mathbf{n}} A_{\mathbf{m}}^\dagger A_{\mathbf{n}} \quad (3)$$

where the $A_{\mathbf{m}}$ are spin-symmetrized composite operators that create or remove singlet or triplet electron/hole pairs in configuration $|\mathbf{m}\rangle = |i_e j_h\rangle$ where $V_{\mathbf{m}\mathbf{n}} = -\langle m_e n_h || n_e m_h \rangle + 2\delta_{S0} \langle m_e n_h || n_e m_h \rangle$ where $S = 1, 0$ is the total spin. [11, 12, 13, 14]

The single particle parameters are taken from Anantram and Mehrez as determined by computing the Coulomb integrals between HOMO and LUMO levels on adjacent base pairs with in a double-strand B DNA sequence using density functional theory (B3LYP/6-31G) [15]. For (dA).(dT), the intrachain electron and hole transfer terms are -0.023 eV and -0.098 eV for the thymidine chain and +0.024 and +0.021 eV along the adenosine chain. The interchain terms are $h_j = 0.063$ eV, $r_j^+ = -0.012$ eV, and $r_j^- = -0.016$ eV for the electron and $h_j = 0.002$ eV, $r_j^+ = -0.007$ eV, and $r_j^- = 0.050$ eV for the hole with site energies $\epsilon_e = -0.931$ eV and $\epsilon_h = -6.298$ eV for the thymidine chain and $\epsilon_e = 0.259$ eV and $\epsilon_h = -5.45$ eV for the adenosine chain. It is important to note that the asymmetry introduced with $r_j^+ \neq r_j^-$ gives directionality between the 3'- and 5'- ends of the chain.

For simplicity, we take the on-site Coulomb interaction $J = -2.5$ eV and the on-site exchange interaction to be $K = 1.0$ eV for both the purines and pyrimidines. We assume these interactions to be local since the distance at which the Coulomb energy between an electron/hole pair equals the thermal energy in aqueous ionic media at 300K is on the order of the base-stacking distance. These

we set as adjustable parameters to tune the predicted absorption spectrum of our model to reproduce the experimental UV absorption spectra. [16] Lastly, we estimated the coupling between geminate electron/hole pairs on different bases $\langle n_e n_h || m_e m_h \rangle$ via a point-dipole approximation by mapping the $\pi - \pi^*$ transition moments onto the corresponding base in the B DNA chain. [20] As in the electron and hole hopping terms, the local dipole-dipole coupling terms read: $d_\perp = -0.099$ eV between adjacent base pairs, $d_\parallel^A = 0.0698$ eV along the adenosine chain, $d_\parallel^T = 0.143$ eV along the thymidine, $d^- = -0.006$ eV for the 5'-5' diagonal coupling and $d^+ = -0.013$ eV for the 3'-3' diagonal coupling. The use of the point-dipole approximation in this case is justified mostly for convenience and given the close proximity of the bases, multipole terms should be included in a more complete model. [17] As a result, the matrix elements used herein provide an upper limit (in magnitude) of the couplings between geminate electron-hole pairs. Most importantly, however, the point-dipole approximation provides a robust means of incorporating the geometric arrangement of the bases into our model. [16] Having briefly discussed the model and how we determined the parameters, we move onto discuss the result of our dynamical calculations.

We consider the fate of an initial singlet electron/hole pair placed either in the middle of the thymidine side of the chain or the adenosine side of the chain (i.e. an exciton). We assume that such a configuration is the result of an photoexcitation at the appropriate photon energy (4.87 eV for the thymidine exciton and 5.21 eV for the adenosine exciton respectively) and based upon the observation that the UV absorption spectra largely represents the weighted sum of the UV spectra of the constituent bases, such localized initial states are Since these are not stationary states, they evolve according to the time-dependent Schrödinger equation. Over a short time-step, δt this is easily computed using the Tchebychev expansion of the time-evolution operator [18]

$$\begin{aligned} \Psi(t + \delta t) &= \exp[-iH(12)\delta t/\hbar] \Psi(t) \\ &= e^{-i\bar{E}\delta t/\hbar} \sum_{n=0}^M a_n(\alpha) T_n(-i\tilde{H}) |\Psi(t)\rangle \quad (4) \end{aligned}$$

$\Delta E = E_{max} - E_{min}$. where $T_n(x)$ are Chebychev polynomials.

$$T_{n+1}(x) = 2xT_n(x) - T_{n-1}(x) \quad (5)$$

with $T_0(x) = 1$ and $T_1(x) = x$. \bar{H} is Hamiltonian operator shifted and scaled so that its eigenvalues lie within $E \in [-1, 1]$, and $J_n(\alpha)$ the n th spherical Bessel function with $\alpha = \Delta E t / 2\hbar$. The advantage of this approach is that converges rapidly, preserves norm, and is computationally efficient since it involves at most matrix-vector multiplications.

In the top two frames of Fig. 2 we show the transient probability for finding an exciton placed on the adenosine

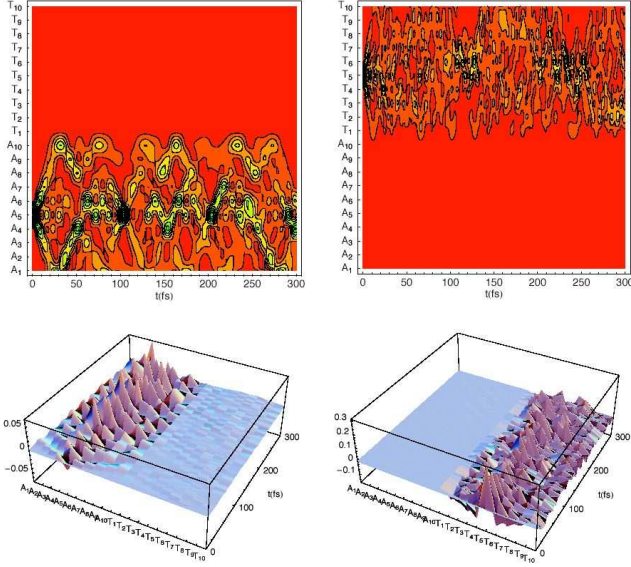


FIG. 2: Top: Time evolution of the exciton density for an initial excitation placed on the adenosine (left) and thymidine (right) chains). Bottom: The corresponding net charge on a given site following excitation of the adenosine (left) and thymidine (right) chains.

(left) or thymidine (right) chain at time $t = 0$ in some other excitonic configuration along either the adenosine or thymidine chain at some time t later. In both cases, negligible exciton density is transferred between chains and the excitons rapidly become delocalized and scatter ballistically down the DNA chain.

There are some striking differences, however, between the exciton dynamics in adenosine versus those in thymidine. First, in comparing the d_{\parallel} matrix elements, one easily concludes that the exciton mobility along the thymidine chain is considerably greater than the mobility along the adenosine chain. This can be seen in Fig 2, comparing the time required for an excitonic wavepacket to reach the end of either chain. In adenosine, the exciton travels 5 base pairs in about 25 fs where as an exciton along the thymidine chain covers the same distance in about 10 fs. This factor of two difference in the exciton velocity is commensurate with the $\approx 1:2$ ratio of the $d_{\perp}^A : d_{\perp}^T$ intrachain excitonic couplings.

Secondly, we note that the adenosine exciton remains qualitatively more “cohesive” than the thymidine exciton showing a number of ballistic traverses up and down the adenosine chain over the 300 fs we performed the calculation. One can also note that the exciton velocity in the 5’-3’ direction is slightly greater than in the 3-5’ direction as evidenced by the exciton rebounds off site A_{10} slightly sooner than it rebounds from site A_1 . This is due to the asymmetry introduced in by the r^{\pm} and d^{\pm} terms. All in all, one can clearly note a series of strong recurrences for finding the adenosine exciton on the original site A_5 ev-

ery 100 fs. The thymidine exciton dynamics are far more complex as the exciton rapidly breaks apart. While few recursions can be noted, however, after the first ballistic traverse, the thymidine exciton no longer exists as a cohesive wavepacket and is more or less uniformly distributed along the thymidine side of the chain.

The excitonic dynamics only tell part of story. In the lower two frames of Fig. 2 we show the net charge taken as the difference between the hole density and electron density on a given base. Note the difference in scale between the bottom left and bottom right figures. In the case where the initial exciton is on the adenosine chain, very little charge-separation occurs over the time scale of our calculation. On the other hand, when the exciton is placed on the thymidine chain, the exciton almost *immediately* evolves into a linear combination of excitonic and charge-separated configurations. What is also striking is that in neither case do either the electron or hole transfer over to the other chain even though energetically charge-separated states with the electron on the thymidine and the hole on the adenosine sides of the chain are the lowest energy states of our model. [16] It is possible, that by including dissipation or decoherence into our dynamics, such relaxation will occur, however, on a time scale dictated by cross-chain transfer terms. For the coupling terms at hand, electron or hole transfer across base pairs occurs on the time scale of 3-4 ps.

The difference between the excitonic dynamics following excitation of A vs. T can be quantitatively noted by comparing the curves shown in Fig. 3 where we compare the projection of the time-evolved state onto the excitonic configurations of the chain on which the exciton was placed (P_{AA} and P_{TT}) compared to the projection onto the excitonic configurations of the other chain (P_{AT} and P_{TA}). For the case in which the adenosine chain was excited, approximately 75% of the total probability density remains as excitonic configurations along the adenosine chain. In stark contrast, only about 40% of the initial thymidine exciton remains excitonic along the thymidine side of the chain. The reason for the remarkable difference between the two chains stems from the difference in electron and hole mobility along the thymidine chain. Indeed, comparing the electron and hole hopping terms given above, $t_h/t_e \approx 4$ for the thymidine chain compared to $t_h/t_e \approx 1$ for along the adenosine chain. This is manifest in the lower right panel of Fig. 2 where we see almost immediately a negative charge remaining for a few fs on the site where the initial excitation was placed.

The results described herein paint a similar picture to that described by recent ultrafast spectroscopic investigations of (dA).(dT) oligomers in that the initial excitonic dynamics is dominated by base-stacking type interactions rather than by inter-base couplings. Interchain transfer is multiple orders of magnitude slower than the intrachain transport of both geminate electron/hole pairs as excitons and independent charge-separated species. Indeed,

for an exciton placed on the adenosine chain, our model predicts that exciton remains as a largely cohesive and geminate electron/hole pair wave function as it scatters along the adenosine side of the chain. Our model also highlights how the difference between the mobilities in the conduction and valence bands localized along each chain impact the excitonic dynamics by facilitating the break up of the thymidine exciton into separate mobile charge-carriers. In the actual physical system, the mobility of the free electron and hole along the chain will certainly be dressed by the polarization of the medium and reorganization of the lattice such that the coherent transport depicted here will be replaced by incoherent hopping between bases.

In conclusion, we present herein a rather compelling model for the short-time dynamics of the excited states in DNA chains that incorporates both charge-transfer and excitonic transfer. It is certainly not a complete model and parametric refinements are warranted before quantitative predictions can be established. For certain, there are various potentially important contributions we have left out: disorder in the system, the fluctuations and vibrations of the lattice, polarization of the media, dissipa-

tion, decoherence, etc. These we recognize as lacunae in our model.

Acknowledgments: This work was funded by the National Science Foundation, the Robert Welch Foundation, and the Texas Center for Superconductivity. The author also wishes to thank Prof. Stephen Bradforth (U. So. Cal.) for many insightful conversations leading to this work.

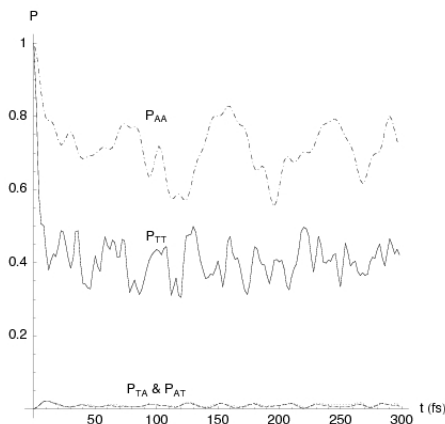


FIG. 3: Net probability, P_{if} for the initial exciton to remain an exciton on the initial chain (P_{AA} & P_{TT}) or to be transferred as an exciton the other chain (P_{AT} & P_{TA})

-
- * email:bittner@uh.edu; URL:<http://k2.chem.uh.edu>
- [1] S. O. Kelley and J. K. Barton, Science **283**, 375 (1999), URL <http://www.sciencemag.org/cgi/content/abstract/283/5400/375>
 - [2] C. E. Crespo-Hernandez, B. Cohen, and B. Kohler, Nature **436**, 1141 (2005).
 - [3] D. Markovitsi, D. Onidas, T. Gustavsson, F. Talbot, and E. Lazzarotto, Journal of the American Chemical Society **127**, 17130 (2005).
 - [4] P. O. Löwin, Rev. Mod. Phys. **35**, 724 (1963).
 - [5] T. Schultz, E. Samoylova, W. Radloff, V. H. Ingolf, A. L. Sobolewski, and W. Domcke, Science **306**, 1765 (2004), URL <http://www.sciencemag.org/cgi/content/abstract/306/5702/1765>
 - [6] E. Emanuele, D. Markovitsi, P. Millie, and K. Zakrzewska, ChemPhysChem **6**, 1387 (2005).
 - [7] E. Emanuele, K. Zakrzewska, D. Markovitsi, R. Lavery, and P. Millie, Journal of Physical Chemistry B **109**, 16109 (2005).
 - [8] D. Markovitsi, F. Talbot, T. Gustavsson, D. Onidas, E. Lazzarotto, and S. Marguet, Nature **441**, E7 (2006), URL <http://www.nature.com/nature/journal/v441/n7094/pdf/nature04411a.pdf>
 - [9] C. E. Crespo-Hernandez, B. Cohen, and B. Kohler, Nature **441**, E8 (2006), URL <http://www.nature.com/nature/journal/v441/n7094/pdf/nature04412a.pdf>
 - [10] M. Creutz and I. Horvath, Nuclear Physics B (Proc. Supp.) **34**, 583 (1994).
 - [11] S. Karabunarliev and E. R. Bittner, The Journal of Chemical Physics **118**, 4291 (2003), URL <http://link.aip.org/link/?JCP/118/4291/1>.
 - [12] S. Karabunarliev and E. R. Bittner, The Journal of Chemical Physics **119**, 3988 (2003), URL <http://link.aip.org/link/?JCP/119/3988/1>.
 - [13] S. Karabunarliev and E. R. Bittner, J. Phys. Chem. B **108**, 10219 (2004), URL <http://pubs.acs.org/cgi-bin/abstract.cgi/jpcbfk/2004/108/i2>
 - [14] S. Karabunarliev and E. R. Bittner, Physical Review Letters **90**, 057402 (pages 4) (2003), URL <http://link.aps.org/abstract/PRL/v90/e057402>.
 - [15] H. Mehrez and M. P. Anantram, Phys. Rev. B **71**, 115405 (2005), URL <http://link.aps.org/abstract/PRB/v71/e115405>.
 - [16] E. R. Bittner, J. Chem. Phys. (submitted) (2006).
 - [17] B. Bouvier, T. Gustavsson, D. Markovitsi, and P. Millie, Chemical Physics **275**, 75 (2002).
 - [18] H. Tal-Ezar and R. Kosloff, J. Chem. Phys. **81**, 3967 (1984).
 - [19] M. W. Schmidt, K. K. Baldridge, J. A. Boatz, S. T. Elbert, M.S.Gordon, J. H. Jensen, S. Koseki, N. Mat-

sunaga, K. A. Nguyen, S. J. Su, et al., J. Comput. Chem **14**, 1347 (1993).

- [20] These are obtained from the isolated bases by performing single configuration interaction (CIS) calculations using the GAMESS[19] quantum chemistry package on the

corresponding 9-methylated purines and 1-methylated pyrimidines after optimizing the geometry at the HF/6-31(d)G level of theory.